



# Fermi National Accelerator Laboratory

FERMILAB-Pub-91/161-A  
June 1991

NAGW-1346  
IN-93-cl

## NON-GAUSSIAN MICROWAVE BACKGROUND FLUCTUATIONS FROM NONLINEAR GRAVITATIONAL EFFECTS

32330

P9

**D.S. Salopek**  
NASA/ Fermilab Astrophysics Center  
P.O. Box 500 MS-209  
Batavia, Illinois, USA 60510

*After October 1, 1991*  
Department of Applied Mathematics and Theoretical Physics  
Silver Street, Cambridge, England CB3 9EW

### ABSTRACT

Whether the statistics of primordial fluctuations for structure formation are Gaussian or otherwise may be determined if the Cosmic Background Explorer satellite (COBE) makes a detection of the cosmic microwave-background temperature anisotropy  $\Delta T_{CMB}/T_{CMB}$ . Non-Gaussian fluctuations may be generated in the chaotic inflationary model if two scalar fields interact nonlinearly with gravity. Theoretical contour maps are calculated for the resulting Sachs-Wolfe temperature fluctuations at large angular scales ( $> 3^\circ$ ). In the long-wavelength approximation, one can confidently determine the nonlinear evolution of quantum noise with gravity during the inflationary epoch because (1) different spatial points are no longer in causal contact, and (2) quantum gravity corrections are typically small— it is sufficient to model the system using classical random fields. If the potential for two scalar fields  $V(\phi_1, \phi_2)$  possesses a sharp feature, then non-Gaussian fluctuations may arise. An explicit model is given where cold spots in  $\Delta T_{CMB}/T_{CMB}$  maps are suppressed as compared to the Gaussian case. The fluctuations are essentially scale-invariant.

in Proceedings of the Fourth Canadian Conference on  
General Relativity and Relativistic Astrophysics  
Winnipeg, Canada, May 16-18, 1991  
ed. G. Kunstatter, World Scientific Publishing Company

(NASA-CR-188699) NON-GAUSSIAN MICROWAVE  
BACKGROUND FLUCTUATIONS FROM NONLINEAR  
GRAVITATIONAL EFFECTS (Fermi National  
Accelerator Lab.) 9 p

N91-31067

CSCL 038

Unclass

63/93 0032330



## 1. INTRODUCTION

With the decline of the Cold Dark Matter scenario, it is imperative that theorists propose alternative models which can be compared with the observations. Here, I describe a variation of the inflation model which yields non-Gaussian primordial fluctuations. This model may be tested in the near future if the Cosmic Background Explorer satellite<sup>1</sup> (COBE) measures the cosmic temperature anisotropy.

Even with the difficulties in accounting for large scale structure, it is still reasonable to retain the inflationary scenario. Redshifts of IRAS galaxies<sup>2</sup> and their inferred peculiar velocities indicate that the Universe is at critical density,<sup>3,4</sup>  $\Omega = \rho/\rho_{crit} = 0.8 \pm 0.3$ . This result gives support to inflation whose most outstanding prediction was that  $\Omega = 1$ . However, one must attempt to modify or improve the scenario so as to produce a set of initial conditions that are richer than scale-invariant Gaussian. Here, I will describe a chaotic inflation model that gives non-Gaussian fluctuations which are basically scale-invariant.<sup>5,6</sup>

There are three essential ingredients to the inflationary scenario. Firstly, a scalar field with potential  $V(\phi)$  models the decay of the cosmological constant. Secondly, gravity is crucial in order to account for the expansion of the Universe. Finally, scalar field quantum fluctuations are necessary to produce inhomogeneities that will eventually produce structure in our Universe. One should view the inflation model as a microscope that magnifies quantum fluctuations at the smallest imaginable distance scales (less than the Planck length) to scales that are cosmologically observable. One of the problems with linear perturbation theory was that there was no short distance cutoff. This gave the illusion that one could extrapolate to arbitrarily small distances. However, nonlinearities must be important at some scale.

Non-Gaussian fluctuations would be the signature of nonlinearities<sup>7</sup> in the inflationary scenario. Their calculation is problematic because one requires a formalism that governs the evolution of quantum noise with gravity. Ideally, one needs a quantum theory of the gravitational field. In order to bypass this very severe difficulty, I will use three tricks:

- (1) The classical nonlinear evolution of long-wavelength scalar fields and gravity is tractable.<sup>8,9</sup> When the wavelength of a fluctuation exceeds the Hubble radius, different spatial points are no longer in causal contact, and they evolve as independent homogeneous universes. One may safely neglect second order spatial gradients in the action for scalar fields and gravity. Nonetheless, one must carefully join the independent spatial points to make one Universe.
- (2) Long-wavelength quantum noise behaves classically, and it may be described using classical random fields in a process termed stochastic inflation.<sup>10,8</sup> Using the Wheeler-DeWitt equation, one may show that quantum gravity corrections are typically small.<sup>8</sup>
- (3) The long-wavelength equations may be solved completely when the logarithm of the scalar field potential is linear,<sup>9</sup>  $\ln V(\phi_j) = \sum_k a_k \phi_k$ , where the  $a_k$  are constants. More complicated potentials may be approximated by joining various linear  $\ln V$  potentials together. In this way, one may produce models that yield non-Gaussian fluctuations that are consistent with current microwave background anisotropy limits.

## 2. LONG-WAVELENGTH FIELDS: GENERALIZATION OF HOMOGENEOUS MINISUPERSPACE

The long-wavelength system is an elegant extension to inhomogeneous fields of homogeneous minisuperspace.<sup>6,9</sup> They enable one to construct non-Gaussian models for structure formation.

Given some initial conditions, I will outline how to solve for the classical long-wavelength evolution of scalar fields  $\phi_j(t, \mathbf{x})$  with potential  $V(\phi_j)$  interacting through gravity. It will be assumed that the metric has the form,

$$ds^2 = -N^2(t, \mathbf{x})dt^2 + e^{2\alpha(t, \mathbf{x})}((dx^1)^2 + (dx^2)^2 + (dx^3)^2), \quad (2.1)$$

which describes an isotropic Universe with inhomogeneous scale factor  $e^{\alpha(t, \mathbf{x})}$ . The lapse function  $N$  is determined when one decides the time hypersurface, although an explicit choice is not necessary. In what follows,  $H(t, \mathbf{x}) \equiv \dot{\alpha}/N$  is the Hubble parameter and  $\pi^{\phi_j}(t, \mathbf{x}) = e^{3\alpha}\dot{\phi}_j/N$  are the momentum densities of the scalar fields.

All second order spatial gradients in the Lagrangian of Einstein gravity with scalar fields will be neglected. It is necessary to retain first order spatial gradients otherwise one returns to homogeneous minisuperspace. The energy constraint,

$$H^2 = \frac{8\pi}{3m_p^2} \left[ \frac{e^{-6\alpha}}{2} \sum_j \pi^{\phi_j^2} + V(\phi_j) \right], \quad (2.2a)$$

and the evolution equations are valid at each comoving spatial point, and they are the same as those for homogeneous flat cosmologies. The new ingredient is the momentum constraint, which joins together the independent spatial points to make one Universe:

$$H_{,i} = -\frac{4\pi}{m_p^2} e^{-3\alpha} \pi^{\phi_j} \phi_{j,i}. \quad (2.2b)$$

The solution of this equation is familiar to those who study fluid mechanics. The Hubble parameter is assumed to be a function of the scalar fields, and the momentum densities are given by partial derivatives with respect to the scalar fields,

$$H \equiv H(\phi_j), \quad \pi^{\phi_j} = -\frac{m_p^2}{4\pi} e^{3\alpha} \frac{\partial H}{\partial \phi_j}. \quad (2.3)$$

When these are substituted into the energy constraint, one obtains the separated Hamilton-Jacobi equation,

$$H^2 = \frac{m_p^2}{12\pi} \sum_j \left( \frac{\partial H}{\partial \phi_j} \right)^2 + \frac{8\pi V(\phi_j)}{3m_p^2}. \quad (2.4)$$

This self-contained equation for the Hubble parameter governs the nonlinear dynamics of the long-wavelength gravitational system. It is covariant in that it does not refer either to the time hypersurface nor to the spatial coordinates.

In a significant improvement for calculations based on Hamilton-Jacobi methods,<sup>9,5</sup> I gave an complete analytic solution of the SHJE for two scalar fields  $(\phi_1, \phi_2)$  interacting with gravity through an exponential potential,<sup>11</sup>

$$V(\phi_1, \phi_2; p, \theta) = V_0 \exp\left[-\sqrt{\frac{16\pi}{p}} \frac{(-\phi_1 \sin\theta + \phi_2 \cos\theta)}{m_p}\right]. \quad (2.6)$$

The coupling parameter  $p$  controls the steepness of the potential whereas  $\theta$  is the angle that surfaces of uniform potential make with the  $\phi_1$  axis. The complete solution for the Hubble parameter depends on two arbitrary parameters,  $b$  and  $m$ ,

$$H \equiv H(\phi_1, \phi_2; p, \theta; b, m), \quad (2.7)$$

and it is shown in Fig.(1). Surfaces of constant Hubble parameter are plotted as solid curves in Fig.(1) for the case  $m = 1$ ,  $\theta = 0$ . The family of orthogonal lines are the physical trajectories. All solutions of the SHJE with potential (2.6) may be derived from this solution.

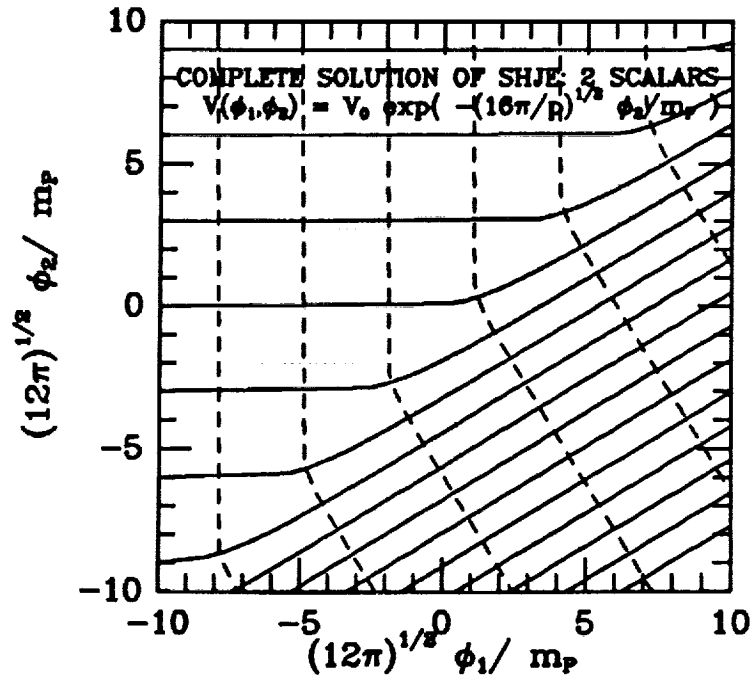


Fig.(1): The complete solution,  $H(\phi; b, m; p, \theta)$ , of the separated Hamilton-Jacobi equation is shown for two scalar fields interacting through a linear  $\ln V$  potential, eq.(2.6). Here, the mixing angle  $\theta$  vanishes, and the constant parameters are chosen to be  $b = 0$  and  $m = 1$ . Surfaces of constant potential are just horizontal lines. The broken lines are trajectories of the fields which move up the page; they are orthogonal to the surfaces of constant Hubble parameter (solid lines).

The complete solution (2.7) generates a transformation to new canonical variables,  $b$ ,  $m$ , with conjugate momenta,  $\pi^b$  and  $\pi^m$ , given by differentiation of the Hubble parameter,

$$\pi^b = \frac{m_p^2}{4\pi} e^{3\alpha} \frac{\partial H}{\partial b}, \quad \pi^m = \frac{m_p^2}{4\pi} e^{3\alpha} \frac{\partial H}{\partial m}. \quad (2.8)$$

The new canonical variables ( $b, m, \pi^b, \pi^m$ ) are constants in time, although they may be spatially dependent. They completely govern the evolution of the system. However, they are not all independent because they are constrained through the new version of the momentum constraint,

$$0 = \pi^b b_{,i} + \pi^m m_{,i}, \quad (2.9)$$

For a single scalar field,<sup>12,8</sup> when the wavelength of the perturbation is larger than the Hubble radius, the system is characterized by a constant of integration,  $\zeta \equiv \zeta(\alpha, \phi)$ . It is the quantity of primary interest for adiabatic models of structure formation. For example, in the Cold Dark Matter Model, microwave background anisotropies at angular scales greater than  $\sim 3^\circ$  are directly proportional to  $-\zeta$ ,

$$\Delta T_{CMB}/T_{CMB} = -\zeta/15. \quad (2.10)$$

This is just the Sachs-Wolfe relation. For multiple scalar fields, eq.(2.10) may be taken as the definition of  $\zeta$ , and using eqs.(2.7,2.8), one may write down an exact expression which is a function of the initial values of the fields,<sup>9</sup>

$$\zeta \equiv \zeta(\alpha_0, \phi_{j0}, \pi_0^{\phi_j}). \quad (2.11)$$

The initial conditions of the long-wavelength problem are generated from short wavelength quantum fluctuations that are assumed to begin in the ground state (Bunch-Davies vacuum). The fluctuations expand beyond the Hubble radius, and they become a part of the long-wavelength background.

### 3. NON-GAUSSIAN MODEL CALCULATIONS

One can obtain non-Gaussian fluctuations on cosmologically observable scales from a potential created by joining three linear  $\ln V$  regions as shown in Fig.(2). It is assumed that our patch of the Universe began homogeneously in the lower half-plane, region 1, where the potential parameters are given by  $p_1 = 20$ ,  $\theta_1 = -50^\circ$ . (For a justification of the homogeneous starting point, see Salopek and Bond.<sup>8</sup>) Short wavelength quantum noise then generates Gaussian initial conditions for the various fields. The broken curves in Fig.(2) depict the subsequent evolution of the scalar fields at several spatial points in a  $64^3$  lattice calculation. When they roll over the various interfaces in the potential, non-Gaussian fluctuations are generated.

The Hubble function,  $H(\phi_j)$ , in region 1 is taken to be the attractor solution,

$$H_{att}(\phi_j) = \sqrt{\frac{8\pi}{3m_p^2} \frac{V_0}{1 - 1/(3p_1)}} \exp\left[-\sqrt{\frac{4\pi}{p_1} \frac{(-\phi_1 \sin\theta_1 + \phi_2 \cos\theta_1)}{m_p}}\right] \quad (3.1)$$

corresponding to  $b = -\infty$  and  $m = 0$  in (2.7) having homogeneous values. The new momentum constraint (2.9) is then satisfied at early times, and the evolution equations guarantee that it will be satisfied at late times. In region 1, the fields then evolve in time  $\alpha$  according to,

$$\phi_1(x, \alpha) = -\frac{m\mathcal{P}}{\sqrt{4\pi p_1}}\alpha \sin\theta_1 + \phi_{10}(x), \quad \phi_2(x, \alpha) = \frac{m\mathcal{P}}{\sqrt{4\pi p_1}}\alpha \cos\theta_1 + \phi_{20}(x), \quad (3.2a)$$

$$\pi^{\phi_1}(x, \alpha) = -\frac{m\mathcal{P}}{\sqrt{4\pi p_1}}e^{3\alpha} H_{att}(\phi_j)\sin\theta_1, \quad \pi^{\phi_2}(x, \alpha) = \frac{m\mathcal{P}}{\sqrt{4\pi p_1}}e^{3\alpha} H_{att}(\phi_j)\cos\theta_1. \quad (3.2b)$$

The initial values of the scalar fields,  $\phi_{i0}(x)$ , are classical Gaussian random fields with power spectrum

$$\mathcal{P}_{\phi_{i0}}(k) \equiv \frac{k^3}{2\pi^2} \langle |\phi_{i0}(k)|^2 \rangle = \left(\frac{H_0}{2\pi}\right)^2 \left(\frac{k}{H_0 e^{\alpha_0}}\right)^{-2/(p_1-1)},$$

whose amplitude is determined by the value of the Hubble parameter  $H_0$  when the lattice size exceeded the Hubble radius. Here,  $H_0 = 10^{-6}m\mathcal{P}$  is chosen to give results consistent with current temperature anisotropy limits. The amplitudes of the homogeneous  $k = 0$  Fourier modes are arbitrary.

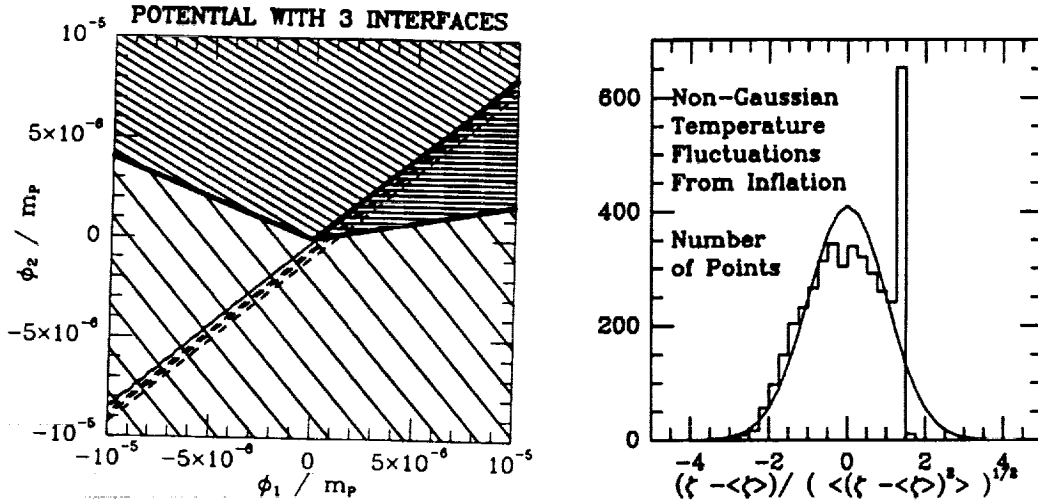


**Fig.(2):** (a) Non-Gaussian fluctuations consistent with CMB limits may be generated when the scalar fields pass over several interfaces in their potential. The light solid curves are lines of uniform potential, whereas the heavy lines are the interfaces which continuously join the 3 regions with linear  $\ln V(\phi_1, \phi_2)$ . If the scalar field trajectories (broken lines) beginning at the bottom of the diagram pass sufficiently near the origin, then nonlinear effects at long wavelengths become important. For a  $64^3$  lattice simulation, the histogram of the resulting fluctuations in  $\zeta$  are shown in Fig.(b). The distribution of microwave background fluctuations at large angular scales is found by reflecting the distribution about the vertical axis:  $\Delta T_{CMB}/T_{CMB} = -\zeta/15$ . For comparison, a Gaussian distribution (smooth curve) with the same mean and dispersion as the histogram is also shown.

If the trajectories pass into the upper right hand area, region 2 ( $\theta_2 = 0^\circ$ ), they receive an upward kick from the potential, which later forces them into region 3 ( $\theta_3 = -30^\circ$ ). (If this diagram were extended, one would find that trajectories actually cross into region 3.) The angles of the interfaces starting with the lower right and proceeding counterclockwise are,  $\chi_{12} = 10^\circ$ ,  $\chi_{23} = 39^\circ$  and  $\chi_{31} = 158^\circ$ . The resulting distribution of  $\zeta$  is plotted in Fig.(2b). For the parameters shown, it was found that non-Gaussian fluctuations can arise if the fields passed sufficiently near the origin, which can be arranged through the arbitrary choice of the homogeneous mode amplitudes in eq.(3.2). The calculations are performed using the analytic expression for  $\zeta$  eq.(2.11).

A 2-D slice of the  $64^3$  lattice simulation is shown in Fig.(3). Large positive excursions of  $\zeta$  are heavily suppressed (i.e. negative excursions of  $\Delta T_{CMB}/T_{CMB}$  are suppressed). With some further analysis, this plot could be interpreted as a large angle microwave background map. The power spectrum for the full 3-D simulation is given in Fig.(4). It is essentially flat.

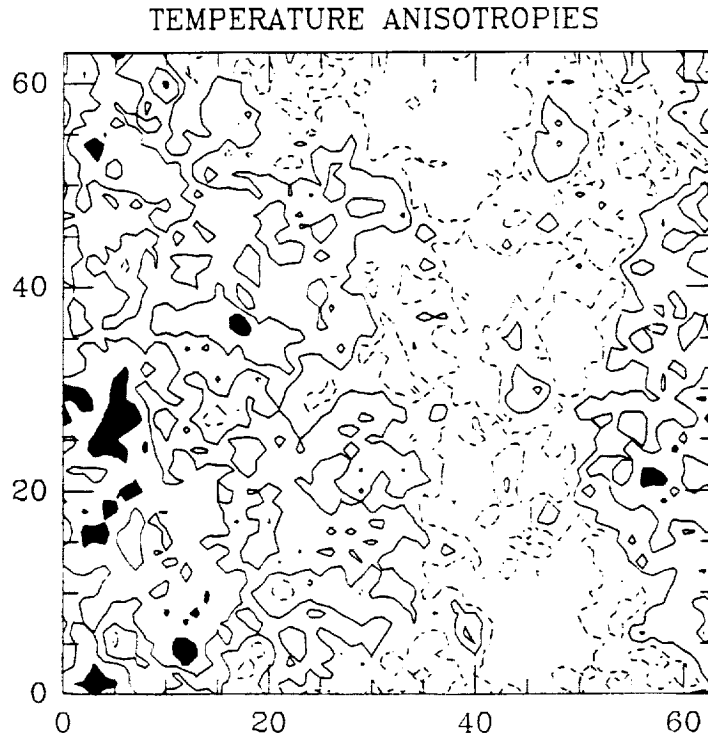


**Fig.(3):** Sachs-Wolfe temperature fluctuations are shown on a 2-D planar slice for the non-Gaussian model considered in Fig.(2). The shaded areas are  $2\sigma$  deviations from the mean for  $\Delta T_{CMB}/T_{CMB}$ . The solid lines correspond to  $1,0\sigma$  contours, whereas the broken lines are  $-1\sigma$  deviations. The most significant feature of this plot is that cold spots in the temperature anisotropy are suppressed over the usual Cold Dark Matter model with Gaussian primordial fluctuations. In fact, there are no  $-2\sigma$  fluctuations of  $\Delta T_{CMB}/T_{CMB}$  in this  $64^3$  lattice calculation, a result which is expected from the distribution function of Fig.(2b).

#### 4. SUMMARY AND DISCUSSION

The distribution of temperature anisotropies could serve as a valuable discriminator of various models of the early Universe. For example, it could indicate that nonlinearities in inflation model were important. It could even determine what was the initial quantum state of the Universe (see, for example, Hartle<sup>13</sup>).

The resulting structure formation scenario for the proposed non-Gaussian model can be described qualitatively. Since the nonlinearities did not change the shape of the primordial fluctuation spectrum in the Newtonian potential (see Fig.(4)), it is natural to assume (at least in the first approximation) that the normalization of the spectrum using the two-point correlation function of galaxies would be the same as the standard Cold Dark Matter model<sup>14</sup> with Gaussian fluctuations. For example, the variance of temperature fluctuations  $\langle (\Delta T_{CMB}/T_{CMB})^2 \rangle$  would be the same. (In fact, the initial value of the Hubble parameter,  $H_0 = 10^{-6} m_P$ , given in Sec. 4 was chosen for this reason.) Differences from standard CDM would appear in the distribution of the fluctuations. Cold spots in the temperature fluctuations would be suppressed as shown in Fig.(3). In addition, I expect that high positive density excursions in the density field will be suppressed.

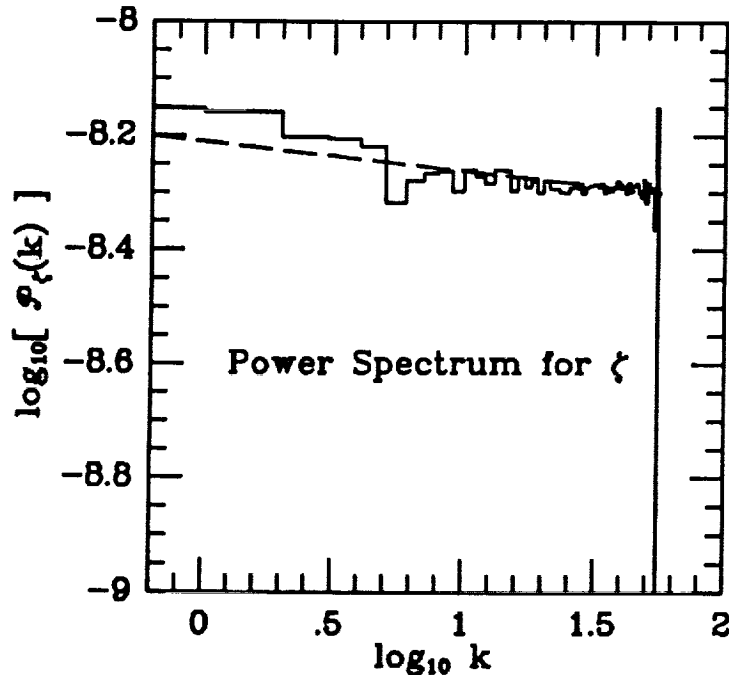


Fig.(4): The power spectrum,  $\mathcal{P}_\zeta(k) \equiv k^3 \langle |\zeta|^2 \rangle / (2\pi^2)$ , for the variable  $\zeta$  is calculated by taking the Fourier transform of the  $64^3$  lattice simulation described in in Fig.(2). Nonlinear effects do not change the shape of the flat spectrum whose amplitude is approximately  $\mathcal{P}_\zeta(k) \sim 10^{-8.3}$ . The comoving wavenumber  $k = 1$  is the largest mode that can fit in the lattice. The slow monotonic decrease for increasing values of  $k$  is a consequence of the



Hubble parameter decreasing in region 1. The larger the potential parameter  $p_1$  of region 1 is chosen, the flatter is the fluctuation spectrum. The spike in the last bin is not significant; it arises because the number of modes in the last bin is small, leading to large shot noise.

There are problems with non-Gaussian scale-invariant fluctuations, or at least with the simple-minded picture adopted above. It is difficult to account for the excess power in the two-point correlation function of galaxies as indicated by the APM survey.<sup>15</sup> However, one should not be overly eager to reject this model because there are observational uncertainties.

I would like to thank N. Kaiser for some interesting discussions. This work was supported by the U.S. Department of Energy and NASA at Fermilab (Grant No. NAGW-1340).

- <sup>1</sup> Smoot, G.F. et al, COBE Preprint (1991).
- <sup>2</sup> Strauss, M.A. and Davis, M., *Large Scale Structure in the Universe, IAU Symposium 130*, eds. J. Audouze and A. Szalay, Reidel, Dordrecht (1991).
- <sup>3</sup> Kaiser, N. and Lahav, O., *Mon. Not. R. Astr. Soc.* **237** 129 (1989).
- <sup>4</sup> Kaiser, N., in this proceedings (1991).
- <sup>5</sup> Salopek, D.S., NATO Advanced Research Workshop: *Observational Tests of Inflation*, Dec. 10-14, 1990, ed. T. Shanks, Kluwer Academic Publishers.
- <sup>6</sup> Salopek, D.S., to be submitted to the *Ap.J.* (1991).
- <sup>7</sup> Allen, T.J., Grinstein, B. and Wise, M., *Phys. Lett.* **B197**, 66 (1987).
- <sup>8</sup> Salopek, D.S. and Bond, J.R., *Phys. Rev.* **D42**, 3936 (1990), **D43**, 1005 (1991).
- <sup>9</sup> Salopek, D.S., *Phys. Rev.* **D43**, 3214 (1991).
- <sup>10</sup> Vilenkin, A., *Phys. Rev.* **D27**, 2848 (1983);  
Starobinski, A.A., in *Current Topics in Field Theory, Quantum Gravity, and Strings*, Proc. Meudon and Paris VI, ed. H.T. de Vega and N. Sanchez **246** 107 (Springer-Verlag, 1986);  
Linde, A.D., *Phys. Lett.* **175B**, 395 (1986);  
Bardeen, J.M. and Bublik, G.J., *Class. Quant. Grav.* **4**, 573 (1987).
- <sup>11</sup> Lucchin, F. and Matarrese, S., *Phys. Rev.* **D32**, 1316 (1985).
- <sup>12</sup> Bardeen, J.M., Steinhardt, P.J. and Turner, M.S., *Phys. Rev.* **D28**, 670 (1983).
- <sup>13</sup> Hartle, J.B., *Gravitation in Astrophysics*, eds. J.B. Hartle and B. Carter, Plenum Press, New York (1986).
- <sup>14</sup> Bond, J.R. and Efstathiou, G., *Ap.J.* **285**, L45 (1984);  
Bond, J.R., in *Proc. of The Early Universe*, ed. W. Unruh and G. Seminoff, Dordrecht: Kluwer (1988).
- <sup>15</sup> Maddox, S.J., Efstathiou, G., Sutherland, W.J. and Loveday, J., *Mon. Not. R. Astr. Soc.* **242**, 43P (1990).

